Natural allelic variations in glutathione peroxidase-1 affect its subcellular localization and function*

Soumen Bera[1,3*], Frank Weinberg[1,*], Dede N. Ekoue[1], Kristine Ansenberger-Fricano[2], Mao Mao[1,2], Marcelo G. Bonini[1,2], Alan M. Diamond[1,]

[1] Departments of Pathology and [2]Medicine, University of Illinois at Chicago, Chicago, IL, USA, [3]Current address: School of Life Sciences, B. S. Abdur Rahman University, Seethakathi Estate, Vandalur, Chennai, TN 600048, India

*Both authors have contributed equally to this publication

Corresponding Author: Alan M. Diamond, Department of Pathology, College of Medicine, 840 S Wood St, University of Illinois at Chicago, Chicago, IL, USA. Tel: (312) 413-8747; Fax: (312) 996-7586; E-mail: adiamond@uic.edu

Keywords: glutathione peroxidase, mitochondria, antioxidant, energy metabolism, selenium

Word count: 5,090
Number of Figures: 7
Number of tables: 0

Abstract

Glutathione peroxidase 1 (GPx-1) has been implicated in the etiology of several common diseases due to the association between specific allelic variations and cancer risk. The most common among these variations are the codon 198 polymorphism that results in either a leucine or proline and the number of alanine repeat codons in the coding sequence. The molecular and biological consequences of these variations remain to be characterized. Towards achieving this goal, we have examined the cellular location of GPx-1 encoded by allelic variants by ectopically expressing these genes in MCF-7 human breast carcinoma cells that produce undetectable levels of GPx-1, thus achieving exclusive expression in the same cellular environment. A differential distribution between the cytoplasm and mitochondria was observed, with the allele expressing the leucine-198 polymorphism and 7 alanine repeats being more cytoplasmically located than the other alleles examined. To assess whether the distribution of GPx-1 between the cytoplasm and mitochondria had a biological consequence, we engineered derivative GPx-1 proteins that were targeted to the mitochondria by the addition of a mitochondria targeting sequence and expressed these proteins in MCF-7 cells. These cells were examined for their response to oxidative stress, energy metabolism and impact on cancer-associated signaling molecules. The results obtained indicated that both primary GPx-1 sequence and cellular location have a profound impact on cellular biology and offer feasible hypotheses as to how expression of distinct GPx-1 alleles can impact cancer risk.

Introduction

Glutathione peroxidase 1 (GPx-1) is the ubiquitously expressed and best characterized member of the glutathione peroxidase (GPx) family of selenium-containing proteins that uses reducing equivalents from glutathione to detoxify peroxides (extensively reviewed in (1)). The translation of GPx-1 includes the recognition of an in-frame UGA triplet as the codon for selenocysteine in a process that requires a selenocysteine insertion sequence (SECIS) in the 3'-untranslated region of the GPx-1 mRNA, a selenocysteine tRNA and a host of selenoprotein-specific translation factors (2-5).

Support for a role for GPx-1 in cancer etiology comes from genetic data indicating significant associations between allelic variations in the GPx-1 gene and cancer risk (6, 7). Two GPx-1 common genetic variations have been extensively studied; a single nucleotide polymorphism resulting in either a proline (pro) or leucine (leu) variation at codon 198 or a variable number of alanine (ala) codon repeats that result in 5,6, or 7 alanines in the amino terminus of the protein (reviewed in (7)). These variations are functional and interactive, determining the levels of GPx-1 enzyme activity for a given concentration of available selenium (8, 9). The *leu* allele has been associated with increased risk of cancers of several types while no clear pattern of association has emerged regarding the number of Ala repeats (7). Recent data demonstrating the interactions between the amino acid at position 198 and the number of alanines may indicate that both variations may need to be considered when conducting studies assessing the role of allelic variations in *GPx-1* as it relates to impacting health outcomes (9). These genetic variations in *GPx-1* are not uncommon, with the proline/leucine-

3

resulting polymorphism exhibiting an approximately 2:1 allele frequency, although the occurrence of the leucine/leucine homozygote genotype is 10% or less (10, 11). GPx-1 alleles encoding 5,6 or 7 alanine-repeat codons in the 5'-terminus of that gene are present at frequencies that are approximately in a 2:1:1 ratio, although individuals homozygous for GPx-1 alleles with either the 5 or 6 codon repeat are uncommon (11, 12). The consequences of these variations on GPx-1 function are not understood, although *in vitro* and human data indicate interactions with enzyme activity and selenium availability, and in one study, gender as well (1).

In order to study the impact of allelic variations in GPx-1, we have taken advantage of the observation that human MCF-7 breast carcinoma cells have negligible GPx enzyme activity and undetectable GPx-1 levels. Previously, we used these cells to exclusively express different GPx-1 alleles by transfection with allelic-specific GPx-1 expression constructs (8, 9). In this manuscript, we used the same approach to further investigate the molecular and biological consequences of allelic variations in the GPx-1 gene to gain a better understanding of the role of GPx-1 in cancer etiology.

Material and Methods

Cell Culture

MCF-7 cells were maintained in modified Eagle's medium (Gibco) supplemented with 10% FBS at 37°C with 5% CO_2. These cells were originally obtained from the American Type Culture Collection and were authenticated by Genetetica DNA Laboratories on July 19, 2013 by analyses of 15 autosomal short tandem repeat loci and the gender identity locus amelogenein. The selenium concentration of the serum used was

determined to be 152 nM by graphite furnace atomic absorption spectrometry conducted at the Texas A&M Veterinary Diagnostic Laboratory at College Station, Texas, resulting in a final concentration of selenium in media containing 10% serum to be 15.2 nM.. Transfectants were generated using the Lipofectamine 2000 transfection reagent (Invitrogen) following the manufacturer's protocol and selected with 500 μg/mL G418 (Sigma), expanded, and screened for GPx-1 activity and expression. Cell survival and proliferation was assayed using the FluoReporter Blue Fluorometric dsDNA Quantitation Kit (InVitrogen).

Generation of allele specific GPx 1 gene constructs

Previously generated GPx-1 expression constructs encoding 5 or 7 alanine repeats at the NH_2 terminus and either a proline or leucine at codon 198 were used as templates to generate mitochondrially targeted variants by fusion of the open reading frames to the mitochondrial targeting sequence (MTS) from the SOD2 gene. A primer containing an 87 nucleotide DNA sequence that included the 72 nucleotide mitochondrial targeting sequence (MTS) from the *SOD2* gene, as well as 15 nucleotides of the 5'-end of the human GPx-1 gene, shown underlined (5'-ATGTTGAGCCGGGCAGTGTGCGGCACCAGCAGGCAGCTGGCTCCGGTTTTGG GGTATCTGGGCTCCAGGCAG<u>ATGTGTGCTGCTCGG</u>-3') was obtained from Integrated DNA Technologies, IA, annealed to the DNA from individual GPx-1 expression constructs and extended using the Klenow fragment. The resulting hybrid DNA was amplified using a *Hind*III containing forward primer (5'-GCAGCAAAGCTTGCAGCATGTTG-3') and a *ClaI* containing reverse primer (5'-

ATAATCGATTGACACCCGGCA-3′). The resulting PCR product was digested with *Hin*dIII and *Cla*1 and directionally inserted into the pLNCX retroviral vector (13).

Subcellular Fractionation

Subcellular fractionation was performed using the standard procedure of Magalhães et al. (14). Briefly, cells were harvested by trypsinization, suspended in ice cold mitochondria isolation buffer (250mM Sucrose, 10mM Tris-Cl, pH 7.4 and 1mM EDTA) and homogenized in a dounce-homogenizer. Efficient lysis was confirmed by viewing images under a light microscope with more than 60% of the cells having been ruptured. The cell lysate was centrifuged at 700 X g for 10 min at 4°C and the resulting supernatant was again centrifuged at 14,000 X g for 10 min at 4°C to pellet mitochondria, which were suspended in the isolation buffer.

GPx activity assay

GPx enzyme activity was determined on whole cell lysates, as well as the mitochondrial and cytosolic fractions, using a coupled spectrophotometric assay that determines the GPx-dependent consumption of NADPH (15). Enzyme activity was expressed as nmole NADPH oxidized per minute per milligram of total protein. In the text, we refer to the cellular activity determined by this assay as "GPx" activity as it cannot be completely ruled out that no other member of the GPxfamily of proteins contributed to the measured activity. For all experiments, cells were plated in triplicate and transfectants were maintained in G418 which was removed from the culture media 2

days before plating the cells to reduce any impact of that antibiotic on selenoprotein synthesis (16, 17).

ROS quantification

Oxidation of the roGFP and mito-roGFP probes was measured by flow cytometry. Briefly, cells were infected with adenoviral vectors expressing roGFP and mito-roGFP sensors at 100 PFU per cell and incubated for 6 hrs after which time the virus-containing media was replaced with complete RPMI 1640 media and incubated overnight. Cells were harvested and equal aliquots were transferred to tubes with media, media with 1mM dithiothreitol or media with 1mM *t*-butylhydroperoxide (*t*-BOOH). After incubation for 10 mins at room temperature, the ratio of fluorescence emission at 535 nm and excitations at 405 and 488 nm was measured in 5,000 cells/sets using a Dako Cytomation CyAn ADP analyzer. The roGFP ratio was obtained by dividing the emission values obtained at 488 nm/535nm by that obtained by 405 excitation/535nm emissions. The oxidation state of the cells was calculated as the difference in the ratio observed with untreated values and completely reduced values divided by the difference in the ratio observed with DTT and t-BOOH. Values are represented as the percentage of oxidation of the probe with 100% being fully reduced and 1% being fully oxidized (18).

Confocal microscopy

Intracellular localization of GPx-1 was verified by confocal microscopy. Briefly, cells were plated on a 1.5mm thick glass bottom culture dish (Mat Tek Corp) and incubated overnight, probed with 200 nM Mitotracker red for labeling mitochondria and

then fixed with 4% paraformaldehyde at 37°C for 30 mins. After fixation, cells were permeabilized and blocked with 3% BSA solution to minimize non-specific binding of the primary antibody. Cells were incubated with a solution containing GPx-1 primary antibody (Aviva) for 45 mins at room temperature followed by incubation with AlexaFluor conjugated secondary antibody for 45 mins at room temperature. Nuclear staining was achieved with 300nM DAPI and cells were imaged using a Zeiss LSM510UV microscope.

Seahorse Extacellular Flux Assay

Cells were plated and grown on Seahorse Bioscience custom plates (North Billerica, MA) in MEM media containing 10% FBS to a uniform monolayer. Cells were then rinsed and transferred to bicarbonate free MEM for 2 hours and then analyzed on the Seahorse Extracellular Flux (XF) Analyzer using the Mitochondria Stress Test Kit. The XF Analyzer measures the oxygen consumption rate (OCR) and the extracellular acidification rate (EACR) (19) at intervals of approximately 2-5 minutes. OCR is an indicator of mitochondrial respiration, and ECAR is predominately the result of glycolysis.

Protein, RNA and enzyme activity analyses

For western blot analysis, protein samples were prepared in NuPAGE® LDS sample buffer (Invitrogen, Grand Island, NY) containing NuPAGE® sample-reducing agent, boiled for 10 minutes, electrophoresed on a 4-12% Bis-Tris denaturing polyacrylamide gel (Invitrogen) and transferred to PVDF membranes. Antibodies against

the following proteins were used: GPx-1 and SBP1 (MBL, International, Woburn, MA), GAPDH and TRXRD (Proteintech, Chicago, IL), Mitochondria complex IV subunit(17 CA) and MnSOD (BD Biosciences, San Jose, CA), GPx4 and β-actin (Abcam, Cambridge, MA), and AKT, pAKT(Ser-473) and NFκB p65 (Cell Signaling, Danvers, MA). Protein bands were quantified using ImageJ software (NIH, Washington, DC) and normalized to β-actin band density.

HPLC detection of superoxide using DHE

For detection of superoxide, cells were washed twice with DPBS and incubated with Hank's Balanced Salt Solution (HBSS) containing 10 µM dihydroethidium (DHE) for 60 mins. Media were collected and centrifuged at 3000 rpm for 5 mins. Fluorescence analysis of the oxidation product 2-hydroxyethidium (EOH) was performed on a Beckman-Coulter HPLC system. Samples were separated on a Synergi-Fusion column (250x4.6 mm, Phenomenex) using a gradient elution of 10% v/v acetonitrile, 0.1% trifluoracetic acid solution (TFA) as the mobile phase A and 100% acetonitrile as mobile phase B with a flow rate set at 1.00 ml/min. Runs began at 100% phase A. Phase B was increased linearly from 0% to 42% in 25 mins, then reduced to 0% during 5 mins and kept at 0% for 5 minutes. The UV detector was set at 350 nm to monitor the elution of DHE. Fluorescence detection was measured using 480 nm (excitation) and 580 nm (emission). Authentic DHE and EOH standard solutions were injected onto the HPLC to determine the retention time of the corresponding peaks. All procedures were performed in the dark or under indirect light. Quantification was performed by normalizing the

integrated peak areas with protein concentrations measured using the BCA Protein Reagent (Thermo Scientific).

Results

Allelic variants of GPx-1 differentially partition between the cytoplasm and the mitochondria

Most studies have focused on the investigation of the cytosolic activities of GPx-1 despite the demonstration that the enzyme also can reside within the mitochondria (20, 21). In order to assess the cellular location of the GPx-1 protein expressed by different alleles, cytoplasmic and mitochondrial cellular fractions were obtained from four previously generated MCF-7 transfectants containing either 5 or 7 alanine repeat codons (A5 or A7) and either a proline (P) or leucine (L) at codon 198, these being referred to as A5L, A7L, A5P or A7P (9). The extracts were analyzed by western blotting with anti-GPx-1 antibodies as well as with anti-COX-1 antibodies as a marker for mitochondrial protein expression. Consistent with several previous publications, GPx-1 was detected in both the cytoplasmic and mitochondrial fractions (20-23). However, this analysis indicated that there was a differential distribution between the cytoplasm and the mitochondria among the proteins encoded by the distinct GPx-1 alleles, with A7L being less distributed to the mitochondria as compared to A5P, A5L and A7P (Fig. 1A and 1B). Pooling data by either the number of alanine repeats or the leucine/proline variation indicated that both genetic variations were contributing to determining cellular localization (Fig. 1C). These results were confirmed by assaying for GPx activity utilizing the same extracts as were used in the western blotting shown in Fig. 1 (Fig. 2).

Thus, quantification of protein levels and the measurement of GPx enzyme activity indicated a differential partitioning of GPx-1 between the cytoplasm and mitochondria, as well as the contribution of both the alanine repeats and the codon 198 polymorphism in determining that distribution.

MCF-7 cells expressing distinct GPx-1 alleles respond differently to oxidative stress

In order to investigate the consequences of allelic variation in the GPx-1 gene on ROS levels, we utilized reduction-oxidation sensitive green fluorescent protein (roGFP) directed to either the cytoplasm or mitochondria (cyto-RoGFP or mito-RoGFP, respectively). These constructs were delivered to cells by viral infection and fluorescence was quantified by flow cytometry. Given the greatest differences among cells expressing distinct GPx-1 genotypes were between those expressing the A5P and A7L alleles, subsequent studies focused on just those two genotypes. The results of this analysis are shown in Fig. 3 and demonstrate that cells expressing the A7L allele, which partitioned to the greatest extent to the cytoplasm, also exhibited the lowest levels of oxidized GFP, both in the cytoplasm (Figure 3A) and the mitochondria (Fig. 3B).

In order to assess whether there were differences in the response of MCF-7 cells expressing those GPx-1 alleles to oxidative stress, cells were exposed to 100 μM *t*-BOOH and consequential changes in growth were assessed over 2 days (Fig.4). Cells expressing A5P were more sensitive to *t*-BOOH than cells expressing A7L ($p<0.05$).

Targeting GPx-1 exclusively to the mitochondria

11

All of the data presented above was conducted with naturally occurring GPx-1 alleles and indicated that the localization of GPx-1 proteins might have a significant impact on the cellular biology of the enzyme. To further investigate this possibility, a hybrid GPx-1 protein targeted to the mitochondria was generated by the fusion of the MnSOD mitochondrial targeting sequence (MTS) to the GPx-1 open reading frame. The constructs encoding the hybrid protein were transfected into MCF-7 cells. Transfectants that expressed the mitochondrially targeted GPx-1 (mito-A5P and mito-A7L) were selected that exhibited similar GPx enzyme activity levels (41.70 ± 1.1 units and 47.16 ± 1.9 units, respectively) and similar to that achieved by the expression of the same two native, non-targeted A5P and A7L alleles (66.47 ± 5.4 units and 49.75 ± 4.5 units, respectively). As seen in Fig. 5A, examination of mitochondrial and cytoplasmic fractions from mito-A5P and mito-A7L expressing cells and examination by western blotting indicated that the targeting was successful and these proteins partitioned exclusively to the mitochondria. Verification of successful targeting was achieved by confocal microscopy using GPx-1 specific antibodies and the Mitotracker Red dye to identify the location of the mitochondria (Fig. 5B).

Both GPx-1 cellular location and primary structure of affect its biological properties

The Seahorse XF24 Extracellular Flux analyzer permits the simultaneous determination of the ECAR (19) which is dominated by lactic acid generated as a result of glycolytic energy metabolism, and the OCR that is a measure of mitochondrial bioenergetic function (24). The relative use of mitochondrial respiration as compared to glycolysis can then be represented as the OCR/ECAR ratio (25). MCF-7 (GPx-1 null),

MCF-7 cells expressing the A5P and A7L GPx-1 isoforms, and MCF-7 transfectants that express those same isoforms exclusively directed to the mitochondria were analyzed using the Seahorse platform (Fig. 6A). The baseline OCR/ECAR ratio was initially recorded, followed by the treatment of the cells with 1.5 μM oligomycin to inhibit complex V of ATP synthase thus disrupting ATP production from the proton gradient. Cells were subsequently exposed to carbonylcyanide-4-(trifluoromethoxy)-phenylhydrazone in order to uncouple respiration resulting in a measure of maximal respiratory rate, a sensitive measure of electron transport chain (ETC) integrity and mitochondrial functional capacity. Finally electron flow through complex I and III were blocked by treating the reaction with rotenone and antimycin A.   The data presented in Fig. 6A surprisingly indicated that both cellular location and the primary amino acid sequence of the GPx-1 isoform affected energy metabolism in these cells, with the mitochondrially directed A7L isoform resulting in mitochondria significantly more active in electron transport as compared to cells expressing the other GPx-1 isoforms.

Next we assessed the effects of GPx-1 cellular location on superoxide levels by measuring the oxidation of DHE by HPLC. Superoxide concentrations were 3 to 4 fold higher when cells expressed GPx-1 (Figure 6B). However, this effect of GPx-1 was significantly diminished when that enzyme was restricted to the mitochondria.

As an additional means of assessing the impact of GPx-1 primary structure and cellular location, cells were treated with *t*-BOOH, and cell viability was determined after 48 hrs by quantifying DNA with the blue-fluorescent Hoechst 33258 nucleic acid stain. As seen in Figure 4, when A7L was directed to the mitochondria, the cells were less protected as compared to the MCF-7 cells expressing that GPx-1 isoform in both the

mitochondria and the cytoplasm (Fig. 4). The consequences of directing A5P to the mitochondria on resistance to *t*-BOOH was less clear given the reduced growth caused by the expression of mitoA5P.

Ectopic expression of GPx-1 isoforms has distinct effects on the expression of signaling proteins and other selenoproteins

It was investigated whether signaling molecules involved in cell growth and metabolism may be differentially affected by the GPx-1 proteins investigated here. Previously, we reported that enhanced GPx-1 expression could alter the phosphorylation of Akt (26), a protein kinase with multiple downstream targets that when activated, can stimulate the switch from oxidative phosphorylation to glycolysis (reviewed in ref. (27)). Increased levels of A5P, mitoA5P, A7L or mitoA7L in MCF-7 cells did not change the levels of total Akt (Fig. 7). Increased expression of A5P dramatically reduced the levels of pAkt, while this was not seen with the mitochondrially targeted protein. In contrast, the expression of A7L increased the phosphorylation of Akt and did so slightly more when located exclusively to the mitochondria (Fig. 7).

GPx-1 down-regulates NFκB, a redox-sensitive transcription factor that impacts cell survival, immunity and other biological processes (28, 29). As expected, over-expression of either A5P or A7L reduced the levels of the NFκB, with this effect being stronger for A7L than A5P. Targeting of those isoforms to the mitochondria had opposing effects: mitoA5P reduced NFκB more effectively than A5P while mitoA7L only marginally reduced NFκB levels.

Lastly, it was investigated whether the cellular location and allelic identity of GPx-1 had an effect on other selenium-containing proteins (Fig. 7). While no effect was observed on the levels of thioredoxin reductase (TrxRD), a selenoprotein critical in maintaining the cellular redox environment, the levels of GPx-4, a membrane-associated member of the GPx family, were affected by both GPx-1 genotype and location. Expression of A5P dramatically reduced the levels of GPx-4 while targeting A5P to the mitochondria also reduced GPx-4 levels, but to a lesser extent. The expression of A7L also reduced the levels of GPx-4 but not to the extent seen with A5P, but in contrast to that seen with A5P, mitoA7L was more effective in reducing GPx-4 levels (Figure 7). Selenium binding protein-1 (SBP1) is a non-selenocysteine containing selenoprotein whose levels are inversely associated with GPx-1 activity and is typically expressed at lower levels in tumors compared to the corresponding normal tissue (30). Expression of either A5P or A7L reduced the levels of SBP1 in MCF-7 cells, although this effect was considerably less when GPx-1 was targeted to the mitochondria (Figure 7).

Discussion

These studies were initiated in order to elucidate the biological consequences of GPx-1 allelic variations and to begin to establish a role for these variations in cancer risk. A role for GPx-1 in determining cancer risk might not be unexpected as a primary function of GPx-1 is to reduce levels of H_2O_2. While more stable and less reactive than other ROS, H_2O_2 might contribute to the direct oxidation of proteins and nucleic acids, or H_2O_2 can be converted into much more reactive ROS, such as the hydroxyl radical by redox active metals. In addition to direct oxidative damage to biomolecules, aerobic

organisms have also evolved to use ROS as potent signaling molecules. Fluctuations in the levels and types of ROS can be due to changes in the cellular microenvironment or intrinsic metabolic adaptations, and examples abound throughout phylogeny indicating the sensing and response to H_2O_2. A significant component of ROS signaling is the consequence of the oxidation of reactive cysteine residues in catalytic proteins and one estimate postulates that over 500 individual proteins might be regulated in this manner, with many being tyrosine and multi-specific phosphatases (31, 32).

A principle result reported in this manuscript was that the selected GPx-1 allelic variants distributed differently between the mitochondria and cytoplasm. The lack of detectable GPx-1 levels in MCF-7 cells made it possible to examine the consequences of the sequence variations in the same cellular environment by ectopically expressing these proteins from expression constructs, thus minimizing the potential contributions of other proteins or factors that might differ across individual cell lines. How GPx-1 partitions to mitochondria remains unknown, particularly as its primary sequence lacks a canonical MTS. The surprising observation that the A7L allele distributed differently than the other variants examined (A5P, A5L, and A7P) indicates that there is an interaction between those variable amino acids located at opposite ends of the protein, perhaps by affecting GPx-1 higher order structure and/or its interaction with other proteins that impact its mitochondrial transport. To date, there is limited information about GPx-1 binding proteins. However, physical interaction with the Abl/Arg tyrosine kinase (33) and selenium binding protein 1, or SBP1 (34) have been reported. The interaction between the alanine repeat motif and the polymorphism at codon 198 may explain the lack of consistency observed among independent epidemiological studies examining the effect of

these variations on cancer risk. To date, there are currently no reports examining associations among cancer risk and both variations in the same population.

The generation of a derivative GPx-1 protein that exclusively partitions to the mitochondria provided direct evidence that the cellular localization of that protein can have a profound effect on cell biology, including resistance to oxidative stress, energy metabolism and signaling. As such, these results provide new evidence for the functionality of these variations and support the existing epidemiological data linking them to disease risk. How the localization of GPx-1 impacts these endpoints remains to be determined. GPx-1 specific enzyme activity may be higher in the mitochondria than the cytoplasm due to its availability for post-translational activation. Recently, two studies have indicated that chronic alcohol consumption and ablation of SIRT3, a mitochondrial deacetylase, leads to hyper-acetylation of several proteins, including GPx-1 (35, 36). Acetylation of GPx-1 was also noted in a recent proteomic analysis that mapped lysine acetylation sites of various proteins across rat tissues and identified 5 potential acetylated lysines in the antioxidant protein (37). It is noteworthy that the GPx-1 allele encoding a leucine at codon 198 is that most often associated with elevated disease risk (7, 38) and may be localized preferentially to the cytoplasm where it would be unavailable for deacetylation and presumed activation by Sirt3. GPx-1 levels and specific activity in the mitochondria may 1) impact the susceptibility of proteins to oxidative damage, 2) influence signaling mediated by the efflux of H_2O_2 generated by the dismutation of superoxide by the mitochondrially located MnSOD protein, or 3) affect the availability of H_2O_2 to serve as a substrate for the recently discovered peroxidase activity of MnSOD (39), resulting in mitochondrial damage, and predisposing to cancer.

17

The complexity of the data obtained by comparing the effects of the different GPx-1 isozymes on both biological and molecular endpoints indicate that both the primary sequence and cellular location impact signaling pathways that may account for the associations between GPx-1 genotype and cancer. The expression of distinct GPx-1 alleles resulted in differences in ROS species that were noted by using roGFP as an indicator of ROS, both in the cytoplasm and in the mitochondria, and differences in superoxide levels were observed using DHE detection. The particular species of ROS and their compartmentalization are likely to contribute to the divergent patterns of activation of signaling pathways, such as those impacted by Akt and NFκB activity seen when different GPx-1 alleles were expressed. GPx-1 has been shown to reduce the transcription of SBP1 as well as to physically interact with that protein (30, 34). It is therefore plausible that the sequestration of GPx-1 in the mitochondria makes it less available to interact with SBP1, a predominantly cytoplasmic protein, or makes it less efficient at reducing H_2O_2 that can stimulate SBP1 transcription via a ROS responsive anti-oxidant response element located 5' to the SBP1 promoter. Collectively, these data provide novel insight into the consequences of GPx-1 genotype and provide plausible mechanisms by which different GPx-1 alleles can contribute to cancer risk.

References

1.   Lubos E, Loscalzo J, Handy DE. Glutathione peroxidase-1 in health and disease: from molecular mechanisms to therapeutic opportunities. Antiox Redox Signal. 2011;15:1957-97.

2.   Berry MJ, Banu L, Chen Y, Mandel SJ, Kiefer JD, Harney JW, et al. Recognition of UGA as a selenocysteine codon in Type I deiodinase requires sequences in the 3' untranslated region. Nature. 1991;353:273-6.

3.   Caban K, Copeland PR. Size matters: a view of selenocysteine incorporation from the ribosome. Cell Molecular Life Sci. 2006;63:73-81.

4.   Driscoll DM, Copeland PR. Mechanism and regulation of selenoprotein synthesis. Annu Rev Nutr. 2003;23:17-40.

5.   Hatfield DL, Gladyshev VN. How selenium has altered our understanding of the genetic code. Mol Cell Biol. 2002;22:3565-76.

6.   Rayman MP. Selenoproteins and human health: insights from epidemiological data. Biochim Biophys Acta. 2009;1790:1533-40.

7.   Zhuo P, Diamond AM. Molecular mechanisms by which selenoproteins affect cancer risk and progression. Biochim Biophys Acta.. 2009;115:227-42.

8.   Hu YJ, Diamond AM. Role of glutathione peroxidase 1 in breast cancer: loss of heterozygosity and allelic differences in the response to selenium. Cancer Res. 2003;63:3347-51.

9.   Zhuo P, Goldberg M, Herman L, Lee BS, Wang H, Brown RL, et al. Molecular consequences of genetic variations in the glutathione peroxidase 1 selenoenzyme. Cancer Res. 2009;69:8183-90.

10. Cox DG, Hankinson SE, Kraft P, Hunter DJ. No association between GPX1 Pro198Leu and breast cancer risk. Cancer Epid Bio Prev. 2004;13:1821-2.

11. Knight JA, Onay UV, Wells S, Li H, Shi EJ, Andrulis IL, et al. Genetic variants of GPX1 and SOD2 and breast cancer risk at the Ontario site of the Breast Cancer Family Registry. Cancer Epid Bio Prev. 2004;13:146-9.

12. Winter JP, Gong Y, Grant PJ, Wild CP. Glutathione peroxidase 1 genotype is associated with an increased risk of coronary artery disease. Coron Artery Dis. 2003;14:149-53.

13. Miller AD, Rosman GJ. Improved retroviral vectors for gene transfer and expression. Biotechniques. 1989;7:980-90.

14. Magalhaes PJ, Andreu AL, Schon EA. Evidence for the presence of 5S rRNA in mammalian mitochondria. Mol Biol Cell. 1998;9:2375-82.

15. Samuels BA, Murray JL, Cohen MB, Safa AR, Sinha BK, Townsend AJ, et al. Increased glutathione peroxidase activity in human sarcoma cell line with inherent doxorubicin resistance. Cancer Res. 1991;51:521-7.

16. Handy DE, Hang G, Scolaro J, Metes N, Razaq N, Yang Y, et al. Aminoglycosides decrease glutathione peroxidase-1 activity by interfering with selenocysteine incorporation. J Biol Chem. 2006;281:3382-8.

17. Tobe R, Naranjo-Suarez S, Everley RA, Carlson BA, Turanov AA, Tsuji PA, et al. High error rates in selenocysteine insertion in mammalian cells treated with the antibiotic doxycycline, chloramphenicol, or geneticin. J Biol Chem. 2013;288:14709-15.

18. Dooley CT, Dore TM, Hanson GT, Jackson WC, Remington SJ, Tsien RY. Imaging dynamic redox changes in mammalian cells with green fluorescent protein indicators. J Biol Chem. 2004;279:22284-93.

19. Eggler AL, Gay KA, Mesecar AD. Molecular mechanisms of natural products in chemoprevention: induction of cytoprotective enzymes by Nrf2. Mol Nutr Food Res. 2008;52 Suppl 1:S84-94.

20. Flohe L, Schlegel W. [Glutathione peroxidase. IV. Intracellular distribution of the glutathione peroxidase system in the rat liver]. Hoppe Seylers Z Physiol Chem. 1971;352:1401-10.

21. Utsunomiya H, Komatsu N, Yoshimura S, Tsutsumi Y, Watanabe K. Exact ultrastructural localization of glutathione peroxidase in normal rat hepatocytes: advantages of microwave fixation. J Histochem Cytochem. 1991;39:1167-74.

22. Esworthy RS, Ho YS, Chu FF. The Gpx1 gene encodes mitochondrial glutathione peroxidase in the mouse liver. Arch Biochem Biophys. 1997;340:59-63.

23. Sies H, Moss KM. A role of mitochondrial glutathione peroxidase in modulating mitochondrial oxidations in liver. Eur J Biochem. 1978;84:377-83.

24. Wu M, Neilson A, Swift AL, Moran R, Tamagnine J, Parslow D, et al. Multiparameter metabolic analysis reveals a close link between attenuated mitochondrial bioenergetic function and enhanced glycolysis dependency in human tumor cells. Am J Physiol Cell Physiol. 2007;292:C125-36.

25. Gohil VM, Sheth SA, Nilsson R, Wojtovich AP, Lee JH, Perocchi F, et al. Nutrient-sensitized screening for drugs that shift energy metabolism from mitochondrial respiration to glycolysis. Nat Biotechnol. 2010;28:249-55.

26.   Nasr M, Fedele MJ, Esser KA, Diamond AM. GPX-1 modulates AKT and P70^{S6K} phosphorylation and GADD45 levels in MCF-7 cells. Free Rad Biol Med. 2004;37:187-95.

27.   Plas DR, Thompson CB. Akt-dependent transformation: there is more to growth than just surviving. Oncogene. 2005;24:7435-42.

28.   Kretz-Remy C, Mehlen P, Mirault ME, Arrigo AP. Inhibition of I kappa B-alpha phosphorylation and degradation and subsequent NF-kappa B activation by glutathione peroxidase overexpression. J of Cell Biol. 1996;133:1083-93.

29.   Li Q, Sanlioglu S, Li S, Ritchie T, Oberley L, Engelhardt JF. GPx-1 gene delivery modulates NFkappaB activation following diverse environmental injuries through a specific subunit of the IKK complex. Antiox Redox Signal. 2001;3:415-32.

30.   Ansong E, Yang W, Diamond AM. Molecular cross-talk between members of distinct families of selenium containing proteins. Mol Nutr Food Res. 2014;58:117-23.

31.   Weerapana E, Wang C, Simon GM, Richter F, Khare S, Dillon MB, et al. Quantitative reactivity profiling predicts functional cysteines in proteomes. Nature.468:790-5.

32.   Finkel T. Signal transduction by reactive oxygen species. J Cell Biol.194:7-15.

33.   Cao C, Leng Y, Huang W, Liu X, Kufe D. Glutathione peroxidase 1 is regulated by the c-Abl and Arg tyrosine kinases. J Biol Chem. 2003;278:39609-14.

34.   Fang W, Goldberg ML, Pohl NM, Bi X, Tong C, Xiong B, et al. Functional and physical interaction between the selenium-binding protein 1 (SBP1) and the glutathione peroxidase 1 selenoprotein. Carcinogen. 2010;31:1360-6.

35. Shepard BD, Tuma DJ, Tuma PL. Chronic ethanol consumption induces global hepatic protein hyperacetylation. Alcohol Clin Exp Res. 2010;34:280-91.

36. Fritz KS, Galligan JJ, Hirschey MD, Verdin E, Petersen DR. Mitochondrial acetylome analysis in a mouse model of alcohol-induced liver injury utilizing SIRT3 knockout mice. J Proteome Res. 2012;11:1633-43.

37. Lundby A, Lage K, Weinert BT, Bekker-Jensen DB, Secher A, Skovgaard T, et al. Proteomic analysis of lysine acetylation sites in rat tissues reveals organ specificity and subcellular patterns. Cell Rep. 2012;2:419-31.

38. Rayman MP. Selenium and human health. Lancet. 2012;379:1256-68.

39. Ansenberger-Fricano K, Ganini D, Mao M, Chatterjee S, Dallas S, Mason RP, et al. The peroxidase activity of mitochondrial superoxide dismutase. Free Rad Biol Med. 2013;54:116-24.

Figure legends

Figure 1. GPx-1 gene polymorphisms affect the cellular distribution between cytosolic and mitochondrial compartments**.** (A) Protein extracts were prepared from cells expressing different GPx-1 alleles and separated into cytoplasmic and mitochondrial fractions. Equal amounts of proteins were electrophoresed and visualized by western blotting with anti-GPx-1 monoclonal antibodies as well as antibodies directed against GAPDH and COX-1 as indicators of cytoplasmic and mitochondrial proteins, respectively. (B) Densitometry was performed on independently prepared extracts with the filled bar representing the signals obtained from the nuclear fraction and the open bars the signals from the cytoplasmic fractions (left panel) and the ratio of the signals obtained from the cytoplasmic to the mitochondrial fractions was determined (right panel). (C) The data was pooled by either the codon 198 polymorphism (proline vs. leucine) or by the number of alanine codons. *P<0.005* for A7L vs. A5P in panel B, of 198P vs. 198L in panel C and 5 alanine repeats vs. 7 repeats with an n=6.

Figure 2. GPx activity in the cytoplasmic and mitochondrial fractions reflects the distribution pattern of the protein expressed from different GPx-1 alleles using the same extracts used to determine the levels of the GPx-1 protein in Fig. 1. (A) Enzyme activity was determined and the ratio of the activity obtained from the cytoplasmic to mitochondrial fractions is presented. The data was pooled by either the number of alanine codons in (B) or the codon 198 polymorphism (proline vs. leucine) in (C). *P<0.005* for

A7L and A7P vs. A5P in panel A, the alanine repeats in panel B or of 198P vs. 198L in panel C and the number of alanine repeats with an n=6.

Figure 3. GPx-1 allelic identity affects ROS generation. MCF-7 cells either transfected with vector or either A5P or A7L were used to assess mitochondrial and cytoplasmic ROS levels using mito-roGFP (A) and cyto-roGFP (B). ro-GFP oxidation was determined by flow cytometry as described in the methods section. *$P<0.005$* vs. MCF vector control with an n=6.

Figure 4. GPx-1 allelic identity affects viability after challenge with ROS. Cells expressing either A5P, A7L, mitochondria-targeted A5P (mitoA5P) or mitochondria-targeted A7L (mitoA7L) were challenged with 100 μM *t*-BOOH for 48 hrs and viability determined. The difference between A5P and A7L following exposure to *t*-BOOH was significant at *$P<0.05$*. The error bars indicate the S.D. with an n=6.

Figure 5. Molecular targeting of the A5P and A7L GPx-1 to the mitochondria. Constructs engineered to express the A5P or A7L GPx-1 alleles were targeted to the mitochondria by attaching the MLS sequence encoded by the mitochondrial MnSOD gene and these constructs were transfected into GPx-1 null MCF-7 cells, selected in antibiotic and expanded for analysis. (A) Protein extracts were prepared, separated into mitochondrial and cytoplasmic fractions and analyzed by western blotting with anti-GPx-1 antibodies. (B) The localization of mitochondrially-directed GPx-1 was confirmed in

individual transfectants by immunhistochemistry and subsequent confocal imaging, where GPx-1 is seen to be exclusively co-localized with mitotracker (red fluorescence) in the transfectants. Nuclei were stained with DAP1 (blue fluorescence).

Figure 6. GPx-1 allelic identity and cellular localization affect mitochondrial metabolism. (A) Oxygen consumption rates were determined in cells expressing either GPx-1 variants or vector using the Sea Horse XF analyzer platform. Data was calculated using the XF Wave software supplied with the analyzer. *$P<0.005$, Ψ $P<0.005$ and $\S$ $P<0.0005$* from MCF7 with n=3. **(B)** The levels of superoxide in MCF-7 transfectants expressing A5P, A7L, mitoA5P or mitoA7L was determined by measuring the oxidation of DHE. The differences between A5P and mitoA5P, and between A7L and mitoA5L was significant at a *$P<0.05$* with a n=3

Figure 7. Expression of GPx-1 isozymes affects the levels of signaling and selenium-containing proteins. Protein extracts were prepared from the indicated cells and analyzed using protein specific antibodies. Actin levels were determined as an indication of equal loading of protein on the gel.
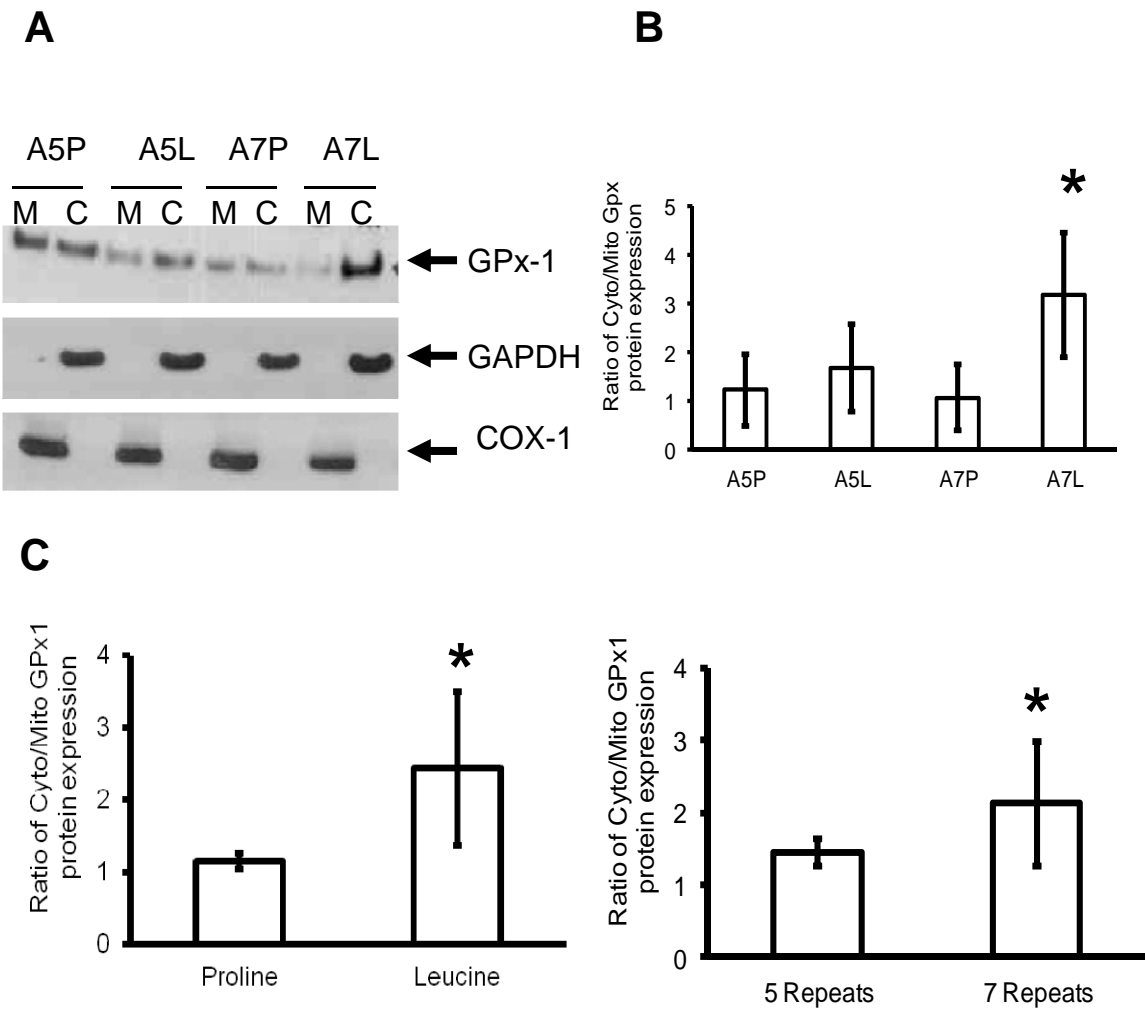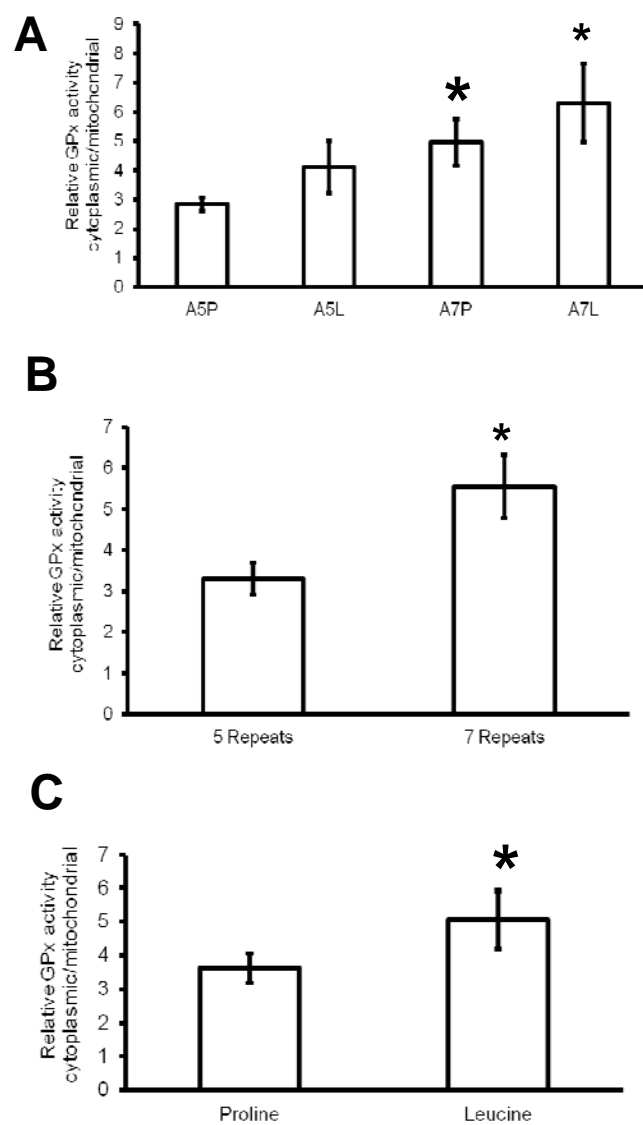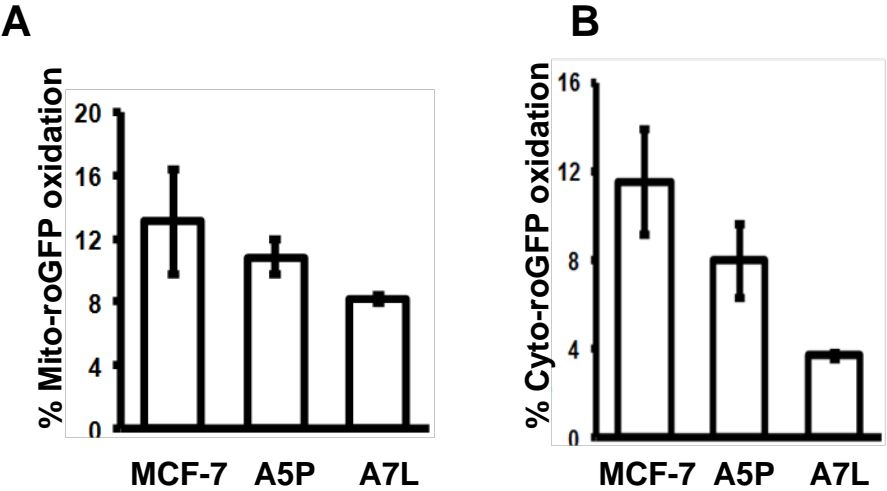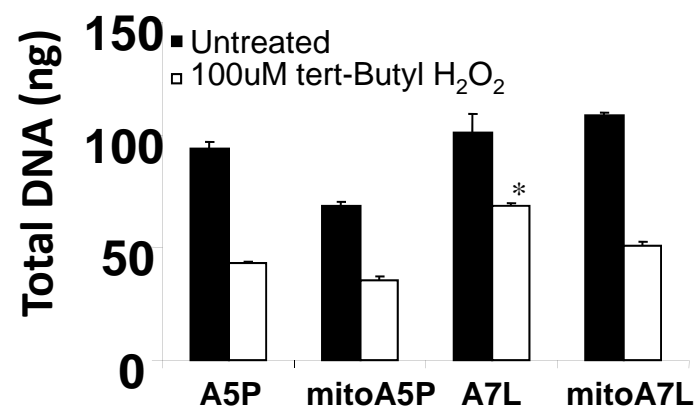
Figure 1

Figure 2

Figure 3

Figure 4

Figure 5

A

	Mito-fraction		Cyto-fraction	
	mitoA5P	mitoA7L	mitoA5P	mitoA7L
GPx-1				
Cox-1				

B

mitoA5P

GPx-1 · CMxROS · DAPI · Overlay

mitoA7L

GPx-1 · CMxROS · DAPI · Overlay

Figure 6

A

B

Figure 7